

Bandstructure and Photoluminescence of SiGe Islands with Controlled Ge Concentration

M. Brehm, T. Suzuki, Z. Zhong, T. Fromherz, J. Stangl, G. Bauer
Institut for Semiconductor and Solid State Physics, University Linz,
Austria

The dependence of the photoluminescence (PL) emission wavelength of SiGe islands embedded into a Si matrix on their Ge concentration and gradient was investigated. Intense PL signals at wavelengths that can be shifted over most of the telecom wavelength range (1.38 – 1.77 μm) by varying the Ge concentration were observed. Using the structural island parameters determined by AFM, TEM and a careful analysis of x-ray reciprocal space maps, good agreement between calculated and measured PL emission wavelength was achieved, indicating that by combining PL and x-ray experiments, an accurate determination of the Ge concentration and a quantitative modeling of the bandstructure of the SiGe islands is possible.

Introduction

Due to its indirect fundamental bandgap in k-space, bulk silicon – the dominating material for microelectronics – is not suitable for optoelectronic applications. Nevertheless, the demand for processing and transmitting a large amount of data in very short times is steadily increasing and intra-chip optical communication links will become more and more important in the near future [1]. Evidently, a Si based optoelectronic platform compatible with modern CMOS technology is highly desirable. Promising sources for light emission in the SiGe system are quantum dots (QDs). It is well known [2] that due to the strain field originating from the QDs, not only holes, but also electrons are bound to the QDs. Due to this confinement, the k-space selection rules are relaxed in all three dimensions. However, while the holes are bound to the Ge-rich region in the interior of the QDs, the electrons are localized in the Si matrix along the surface of the QDs. Thus a spatial indirect (type II) band alignment results and optical interband matrix elements are expected to be small. For optimizing the emission efficiency, a detailed understanding of the bandstructure and its dependence on the structural parameters of the SiGe dots is a prerequisite. In this work, we focused on the influence of the Ge content and its gradient along the growth axis on the emission wavelength and efficiency. Samples containing a single layer of SiGe QD were grown by solid source MBE in the cleanroom of the University Linz. For the Si buffer and QD layer, a growth temperature (rate) of 650 °C (1 Å/s) was used. On top of the buffer, a SiGe alloy layer with the target Ge concentration x_b for the base of the QD was deposited. The Ge flux was kept constant until 3D island nucleation was observed in the RHEED pattern and then ramped up/down in order to reach the desired Ge concentration x_t at the top of the QD. After QD growth, part of the wafer was covered by a shutter during the growth of the 150 nm Si capping layer. The capping layer growth started with a growth temperature (rate) of 450 °C (0.5 Å/s) and was ramped up after 10 nm to 650 °C (1 Å/s). TEM, AFM, and x-ray diffraction were used to investigate the structural parameters of the SiGe islands. These parameters served as input for calculating the bandstructure of the islands by the *nextnano* code [3]. From the bandstructure, the emission energy of the islands is calculated and compared to the photoluminescence (PL) spectrum measured at 10 K

under excitation with an Ar-ion laser at a wavelength of 514 nm and an intensity of 5 W/cm².

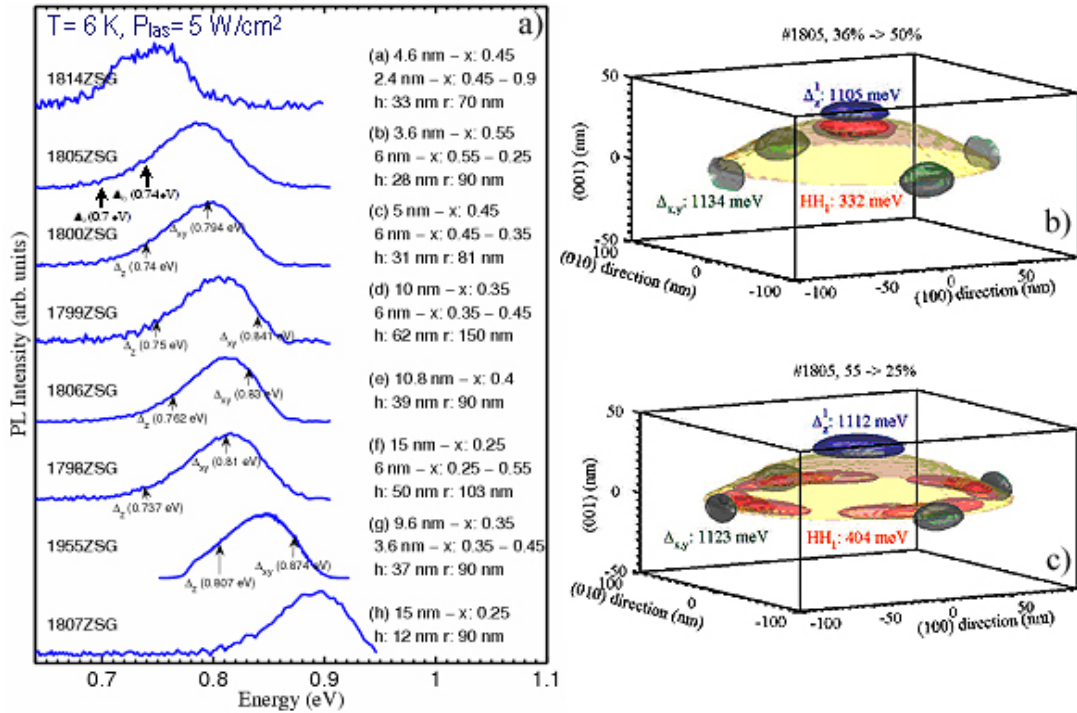


Fig. 1: (a) Measured PL spectra for SiGe islands with nominal structural parameters indicated in the plot. In b), c) the bandstructures for paraboloidal island (r: 90 nm, h: 28 nm) are compared for two different linear Ge gradients ((b) 36→50%; (c) 55→25%). The island surface is shown in yellow, the blue, green and red surfaces confine the regions in which $|\Psi_{\Delta z}|^2$, $|\Psi_{\Delta xy}|^2$, $|\Psi_{HH}|^2$ are larger than 3% of their maximum. The holes are concentrated in the regions of the islands with maximum Ge concentration. The ring-like shape of the HH wavefunction in c) is caused by the strain in the island.

Results and Discussion

The part of the sample covered with a shutter during capping layer growth was used for measuring the dimensions of the QDs by AFM. Paraboloidal islands with base radii and heights between 70–150 nm and 12–60 nm, respectively, as indicated in Fig. 1(a) are observed depending on x_b and x_t . The inter-island distance is typically a few nm in these samples. In Fig. 1(a), the measured PL spectra are shown. For all samples, an intense PL band is observed, the spectral position of which can be adjusted within the telecom range from 0.7 eV (1.77 μ m) to 0.9 eV (1.37 μ m) by the Ge content of the islands. The samples shown in Fig. 1(a) were grown with an intentionally varied Ge concentration during the growth of the islands. By establishing this gradient we tried to investigate the influence of the position of the electrons and holes in their respective groundstates on the luminescence efficiency and energy of the samples. As an example, the dependence of the groundstate positions on the Ge gradient is shown in Figs. 1(b) and 1(c) for sample 1805. For two different Ge gradients (55 to 25% (nominal, Fig. 1(c)), 36 to 50% (Fig. 1(b))) the groundstate wavefunctions for the electrons and holes as calculated by nextnano [3] are shown in a 3D isosurface plot. Here, the red, green and blue surfaces confine the spatial regions, within that the groundstate

$|\psi|^2$ for the heavy holes (HH), the electrons in the Δ -valleys oriented perpendicular (Δ_{xy}) and parallel (Δ_z) to the growth direction, respectively, are larger than 3% of the $|\psi|^2$ maximum. For isolated islands, the calculations show that the electron ground state with the lowest energy is the Δ_z state. A gradient with more Ge at the base than at the apex localizes the HH groundstate at the base (see Fig. 1(c)), resulting in an unfavorable configuration with vanishing overlap of the electron and hole groundstate wavefunctions. On the other hand, the overlap between the energetically higher lying Δ_{xy} states with the heavy hole (HH) groundstate is enhanced in this situation, and radiative Δ_{xy} – HH recombination seems to be more likely than Δ_z – HH recombination, given that the non-radiative lifetime in the Δ_{xy} states is large enough for a sufficiently large metastable electron population to be established there. The arrows shown in Fig. 1(a) indicate the calculated Δ_z – HH and Δ_{xy} – HH transition energies that were obtained by using the nominal structural parameters in the nextnano [3] calculations. It is evident that for all samples shown in Fig. 1(a) the calculated energy difference between the Δ_z – HH and Δ_{xy} – HH transitions is smaller or comparable to the observed inhomogeneously broadened width of the PL emission band. Thus, from comparing these data to the calculated transition energies, it is not possible to identify which transition (Δ_z – HH or Δ_{xy} – HH) is observed. Most probably, the broadening of the PL emission bands is due to a statistical variation of the island size and distance (the influence of the island distance will be discussed in the following). Also the observed shift of the PL line for the various samples is smaller than the calculations based on the nominal structural island parameters indicate. In order to determine the actual structural parameters, and to check whether the designed Ge gradient was correctly established in our growth process, extensive x-ray experiments were performed. In these experiments, we concentrated on the pair of samples with the largest gradient in opposite directions (#1805 and #1798). X-ray diffraction around the 004 and 224 reciprocal lattice points were performed at the beam line BW2 of Hasylab (Hamburg). For various assumed parameter sets for the Ge gradient and for the inter-island distance (the island dimensions were determined by AFM and TEM measurements), the strain distribution in the samples was calculated by finite element (FEM) calculations. Using the results of the FEM calculations, the x-ray intensity around the (115) reciprocal space points was calculated and compared to the measured reciprocal space maps. The best agreement between simulated and measured x-ray maps was achieved assuming that the lateral inter-island distance approaches zero. Under this assumption, for several combinations of x_b and x_t equally good agreement between simulated and measured maps can be obtained. For sample 1805, the range of x_t and x_b for that x-ray fits have been performed, is shown on the abscissa of Fig. 2 (a) together with the nominal parameters (left end of axis) that are not compatible with the x-ray data. The gradients shown at the centre of the axis result in significantly better fits than the gradients on both ends of the axis. Large deviations from the nominal parameters follow from the x-ray analysis indicating that it is difficult to control the Ge gradient during the island growth. As an example for a good fit, the result of the x-ray simulation for sample #1805 assuming a linear gradient from $x_b = 40\%$ to $x_t = 38\%$ is shown by the contour lines in Fig. 2(b) superimposed over the experimental data. For the combinations of x_b and x_t shown in Fig. 2(a), nextnano³ energy band calculations have been performed. The calculated Δ_{xy} –HH and Δ_z –HH PL transition energies are shown by the green and blue symbols in Fig. 2(a). For the Δ_{xy} –HH transition, the results for two assumed lateral inter-island distances (infinity, 2 nm) are shown (light and dark green symbols). The calculations show that the Δ_{xy} –HH transition energy is sensitive to the inter-dot distance. This is because the energy of the Δ_{xy} -states is determined by the compressive strain in the Si around the base of the island. This energy is lowered if the strain fields of adjacent islands start to overlap. The dependence of the Δ_{xy} -HH transition energy on the lateral dot distance is shown in the inset of Fig. 2(a) for sample #1805 with an assumed Ge gradient of 40-38%. For this sample, the Δ_{xy} states become the electron states with the lowest energy

at an inter-island distance below ~ 10 nm. The measured energy and FWHM of the PL line observed for sample #1805 are indicated by the full and broken red lines in Fig. 2(a). For an assumed inter-dot distance of 2 nm, good agreement between calculated and measured PL transition energies is obtained for those gradients, for which also the x-ray simulations result in the best fits (40% – 32%, 40% – 38%). The other gradients shown in Fig. 2(a), for which the nextnano [3] results also agree reasonably with the measured PL energy, produce no reasonable correspondence between measured and simulated x-ray data.

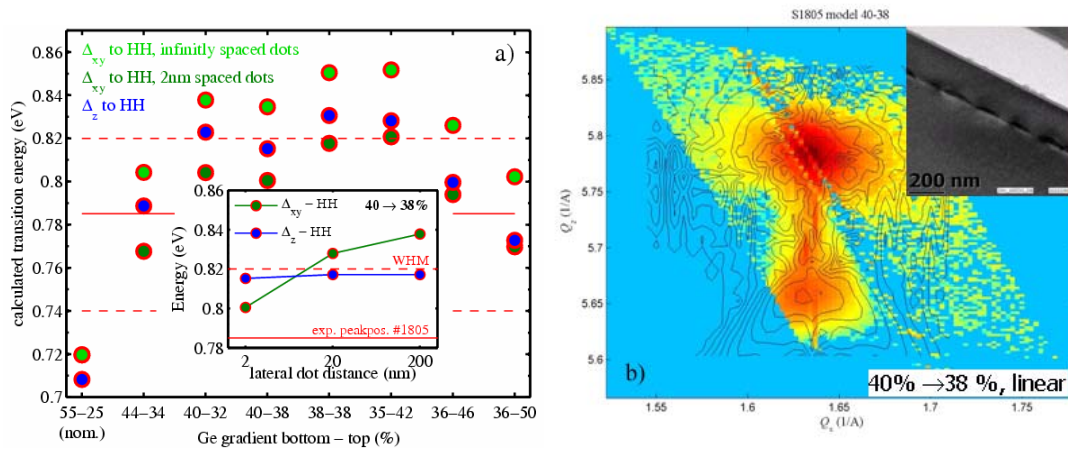


Fig. 2: (a) Calculated PL energies using the dimensions of sample 1805 and the Ge gradients indicated on the abscissa. Blue (green) symbols indicate the calculated $\Delta_z \rightarrow \text{HH}$ ($\Delta_{xy} \rightarrow \text{HH}$) transition energies. Dark (light) green symbols indicate results for 2 nm (∞) spaced islands. Inset: Dependence of the calculated PL energies on the island separation for islands with 40% → 38% Ge gradient in more detail. The full (broken) red lines show the measured peak position (FWHM). (b) Measured (color) and simulated (full lines) x-ray reciprocal space map for sample 1805. The good fit shown was obtained for a Ge gradient of 40% → 38% and vanishing island spacing. Inset: TEM picture of sample 1805.

Summary

Intense PL bands are observed for single layer SiGe islands with intentionally varied Ge content grown by MBE. Depending on then Ge content, the PL emission wavelength is observed at various wavelengths covering the whole technologically important telecom wavelength range. From both the simulation of x-ray reciprocal space maps and the calculation of PL transition energies based on the nextnano [3] code, the Ge concentration and its gradient within the islands can be determined consistently. The obtained results strongly deviate from the nominal values, indicating that a tight control of the Ge gradient in the islands is a difficult task. In addition to the variation of the island size, the statistical variation of the inter-island distance is identified as a source of inhomogenous PL line broadening.

Acknowledgements

This work was supported by the FWF (SFB IRON, Proj. Nrs. F2512-N08, F2507-N08).

References

- [1] http://mph-roadmap.mit.edu/about_ctr/report2005/5_ctr2005_silicon.pdf
- [2] O. Schmidt, Phys. Rev. B **62**, 16715 (2000).
- [3] <http://www.wsi.tu-muenchen.de/nextnano3/index.htm>